Rev. Adv. Mater. Sci. 33 (2013) 291-297

SIMULATION OF METAL DROPLET EVENTS DURING GAS HORIZONTAL ATOMIZATION STAGE IN THE SPRAY ROLLING OF 7050 ALUMINUM ALLOY

Fengxian Li, Yunzhong Liu, Wenhua Xiao and Jinle Xie

National Engineering Research Center of Near-net-shape Forming Technology for Metallic Materials, South China University of Technology, Guangzhou 510640, China

Received: October 17, 2011

Abstract. Spray rolling is a novel metallic semi-solid near-net-shape forming technology. This paper describes the qualitative influence of the key process parameters on the history of velocity, dynamic behavior and enthalpy of the gas and atomized droplets in spray rolling of 7050 alloy based on the fundamentals of spray forming and twin-casting. Results show that the process parameters such as flight time, gas initial velocity, droplet diameter, metal mass flow rate have remarkable influence on process performance including the heat transfer coefficient, droplet velocity, temperature, and solid fraction. This work provides a method to better understand the spray rolling technology.

1. INTRODUCTION

The technology of spray rolling (as shown in Fig. 1), which is complex and involves multi-phase fluid flow, rapid solidification and consolidation, combines powder production, consolidation, and rolling into a single step. Moreover, it is beneficial because of spray rolled products' microstructure refinement such as equiaxed grain structures and excellent mechanical properties with low cost. Compared with the conventional ingot metallurgical processes such as ingot casting, homogenization, hot rolling and twin-rolling strip casting, spray rolling can reduce manufacturing cost while improving quality, keeping high production rate and processing a broad range of alloys [1,2]. Presently, spray rolling is successfully used to process a wide verity of Al alloys such as 2124, 7050, 6111 [3,4].

Published papers about spray rolling technology [5-9] reveals that the laboratory-scale strip caster at Idaho National Engineering and Environmental Laboratory has been used to produce strips. S.B. Johnson and J.-P. Delplanque developed a numerical model which includes atomizing gas flow, in-flight droplet behavior and impact droplet behavior and oxide breakup to study the spray rolling process, but they modeled thermal energy transfer only within a single droplet. The heat transfer of droplets in spray rolling of 7050 aluminum alloy, in many cases, has not been understood. This paper extends the model of thermal and solidification history of a representative droplet and studies key process parameters by means of simulation which can provide insight into the mechanisms controlling process performance for the purpose of process optimization and predict the properties based on process parameters.

2. THEORETICAL MODELS

During spray rolling, a molten aluminum alloy metal stream is atomized into droplets(20~200 μm) by the impact of inert gas with high energy in the horizontal direction, the droplets are collected and deposited

Corresponding author: Yunzhong Liu, e-mail: yzhliu@scut.edu.cn

© 2013 Advanced Study Center Co. Ltd.

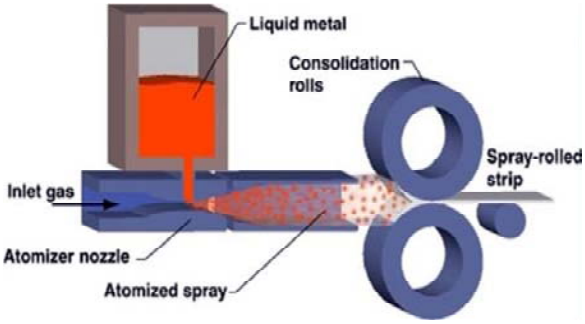

Fig. 1. Schematic of spray rolling, replotted from [1].

between the roll gaps of the twin-roll, and finally rolled to form aluminum strip [10-15].

2.1. Droplet velocity

In spray rolling, the velocity of droplet includes the horizontal movement due to the drag force by gas jet and vertical movement by the gravitation force and buoyancy. Because the flight time is short and the horizontal component of particle velocity is much larger than the vertical component, the gravity effect can be neglected. Following the Newtonian momentum equation, the droplet velocity can be described as follows [16,17]:

$$\frac{dv_d}{dt} = -\frac{3}{4}\frac{1}{d}\frac{\rho_g}{\rho_d}C_{drag}\left[v_d - v_g\right]\left(v_d - v_g\right), \quad (1)$$

where v_d and v_g are the axial direction velocity of droplet and gas, $v_g(z,0) = v_0\exp(-z/\lambda_v)$ [18-19], v_0 is the initial gas velocity, λ_v is the gas velocity decay coefficient, ρ_d and ρ_g are the density of the droplet and gas, C_{drag} is the drag coefficient [20]. At first, we can choose the droplet with a median diameter to represent all droplets for calculation in the whole process.

2.2. The thermal history of in-flight droplets

Cooling and solidification behavior of in-flight droplets has been extensively investigated via numerical analysis that can be directly utilized to analyze in-flight droplets during spray rolling [5,21]. Investigators have suggested that the cooling behavior of an atomized droplet can be divided into five different thermal regions [18-20]. In this system containing partial solid phase, the heat extraction by convection and radiation can be expressed as follows [19, 22-24]:

$$\frac{dH}{dt} = C_d\frac{dT_d}{dt} - \Delta H_f\frac{df_s}{dt} = \frac{6h}{\rho_d d}\left(T_d - T_g\right) - \frac{6\varepsilon\sigma}{\rho_d d}\left(T_d^4 - T_w^4\right), \quad (2)$$

where $C_d = C_L - (C_L - C_S)f_s$ and $\Delta H_d = \Delta H_f - (C_L - C_S)(T_L - T_d)f_s$, here C_d, C_L, C_s are the heat capacity per unit mass of liquid-solid mixture, liquid and solid, respectively, ΔH_f is the latent heat per unit mass and T_L is the liquid temperature, T_d is the droplet temperature, T_g the gas temperature and T_w the temperature of the surrounding walls. And ε, σ are the emissivity and Stefan–Boltzmann constant, the heat transfer coefficient, h, given from Ranz-Marshall correlation [16,23,25,26]:

$$h = \frac{k_g}{d}\left(2.0 + 0.6Re^{1/2}Pr^{1/3}\right), \quad (3)$$

where K_g is the gas thermal conductivity, Pr is the gas Prandtl number.

The liquid cooling stage: The droplets are completely molten. The cooling equation can be described as:

$$\frac{dH}{dt} = C_L\frac{dT_d}{dt}. \quad (4)$$

When the droplet temperature reaches the liquidus of the material, undercooling may take place before the nucleation, which depends on the cooling rate and droplet size. The droplet will not solidify immediately, so Eq. (4) is still valid.

Recalescence stage: The droplet temperature has a sharp increase due to the release of latent heat. The thermal balance equation during recalescence can be described as follows.

$$\frac{dH_d}{dt} = C_d\frac{dT_d}{dt} - \Delta H_d\frac{df_s}{dx}K_i\left(T_L - T_d\right). \quad (5)$$

Assuming nucleation takes place at the surface of the droplets, the solid fraction in this stage is given [16]:

$$\frac{dH_d}{dx} = \frac{1}{d}\left[3\left(\frac{x}{d}\right) - \frac{1}{2}\left(\frac{x}{d}\right)^2\right]. \quad (6)$$

The velocity of the solid–liquid interface movement is approximated as: $dx/dt = K_{sl}\Delta T$, Where K_{sl} is the liquid- solid interface mobility taken as 0.02 $ms^{-1}K^{-1}$ in the present study [24].When recalescence ends, the droplet temperature T_d is equal to T_r, and T_r can be calculated in Eq. (7).

Table 1. Thermo physical properties of 7050 and N_2.

7050 Aluminum alloy				Nitrogen gas N_2	
ΔH_f	257500 [Jkg^{-1}]	TM	933 [K]	ρ_g	1.138 [kgm^{-3}s^{-1}]
C_{ps}	860 [Jkg^{-1}K^{-1}]	TL	908 [K]	μ_g	1.873*10^{-5} [Nsm^{-2}]
C_{pl}	1029 [Jkg-1K-1]	TE	738 [K]	K_g	0.0258 [Wm^{-1}K^{-1}]
ρ_d	2820 [kg m-3]	γ_m	0.914-3.5e-4(T-Ti) [N m^{-1}]	C_{pg}	1043.21 [Jkg^{-1}K^{-1}]
K_e	0.166	μ_m	1.429e-4exp(16500/8.3144/T) [Nsm^{-2}]	–	–

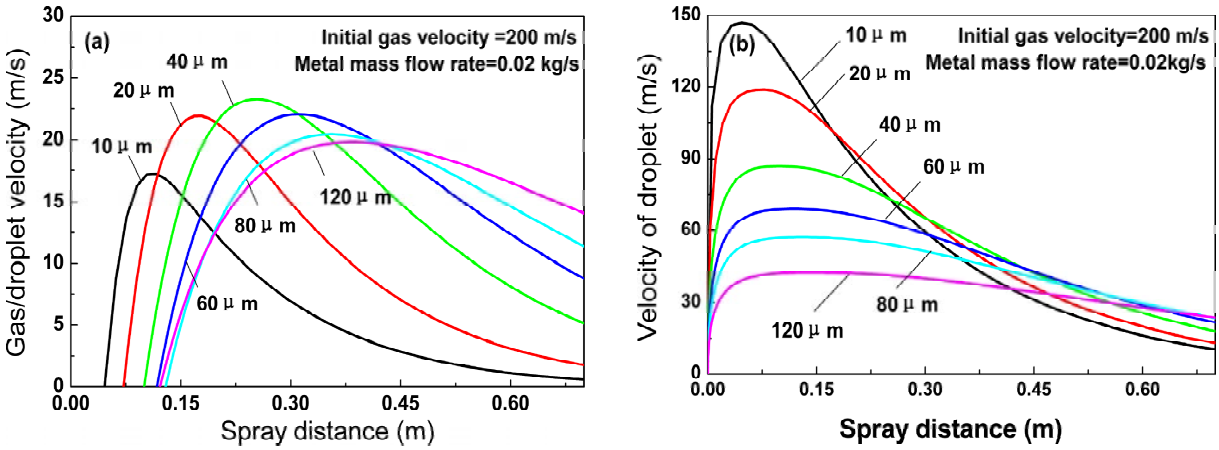

Fig. 2. Variations of gas /droplet slip velocity (a) and droplet velocity (b) with spray distance for different droplet diameters.

$$\left[\Delta H_f - \left(C_L - C_s\right)\left(T_L - T_R\right)\right]\frac{\mathrm{d}f}{\mathrm{d}t} = -\frac{6h}{\rho_d d}\left(T_R - T_g\right). \quad (7)$$

Segregated solidification: after the recalescence, the heat exchange can be also expressed as Eq. (8). According to Scheil's equation [27], the changing rate of f_s with T_d can be described as follows.

$$\frac{\mathrm{d}f}{\mathrm{d}T_d} = \frac{1-f_r}{\left(k_e - 1\right)\left(T_M - T_{d,r}\right)}\left(\frac{T_M - T_r}{T_M - T_{d,r}}\right)^{\frac{2-ke}{1-ke}}. \quad (8)$$

Eutectic solidification: in this stage, the droplet temperature remains at a constant value, the eutectic temperature T_E, until the phase transformation is terminated. The solidification can be evaluated from Eq. (9).

$$\left[\Delta H_f - \left(C_L - C_s\right)\left(T_L - T_R\right)\right]\frac{\mathrm{d}f}{\mathrm{d}t} = -\frac{6h}{\rho_d d}\left(T_E - T_g\right). \quad (9)$$

Further cooling behavior after eutectic solidification is the same as the segregated solidification and the solid fraction increases to 1. The cooling equation in the solid stage is given as the following:

$$\frac{\mathrm{d}H}{\mathrm{d}t} = C_s\frac{\mathrm{d}T_d}{\mathrm{d}t}. \quad (10)$$

2.3. Thermo-physical properties of materials

The thermo-physical properties of 7050 alloy and nitrogen (atomizing gas) were shown in Table 1 [28].

3. NUMERICAL RESULTS AND DISCUSSION

3.1. Effects of droplet size

Fig. 2 shows the changes of droplet velocity, droplet /gas velocity respectively for 7050 alloy droplets of 10, 20, 40, 60, 80, and 120 μm with an atomizing gas of N_2, as a function of spray distance. Gas / droplet slip velocity is defined as the velocity of droplet minus the velocity of gas. At the beginning,

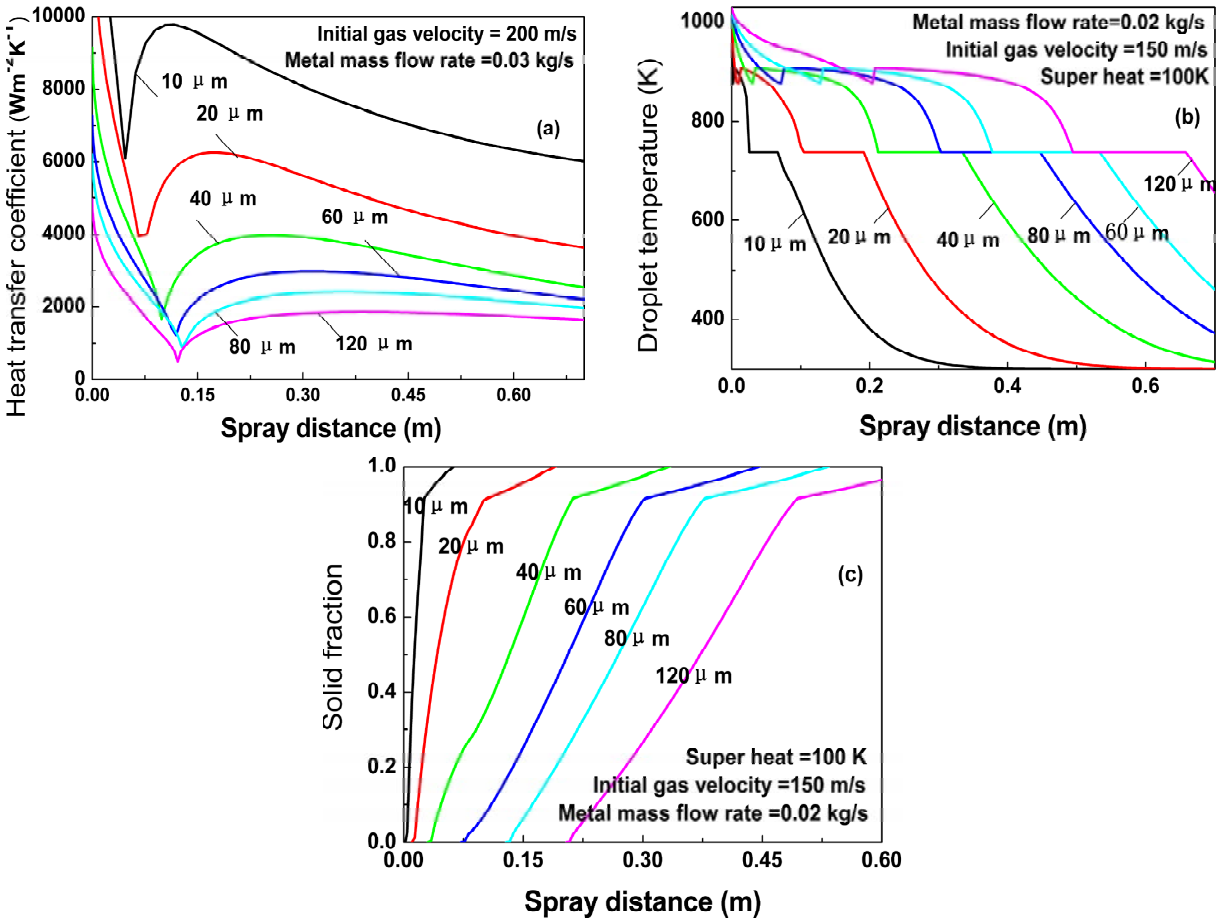

Fig. 3. Variations of heat transfer coefficient (a), temperature (b), and solid fraction (c) with flight time for different droplet diameters.

gas /droplet slip velocity is equal to the initial velocity of gas in Fig. 2a. All the droplets are firstly accelerated by the gas then decelerated. As shown in Fig. 2b, a small droplet is effectively accelerated to a higher maximum velocity in a shorter flight distance than a large droplet. For example, the maximum velocity for the droplet of 10 μm diameter is 118.96 m/s, while it is 42.53 m/s for the droplet of 120 μm diameter. Meanwhile the spray distance for a droplet of 10 mm decreases by about 0.047 m compared with that for a droplet of 120 μm. It was found that small droplets are more sensitive to gas velocity.

The relationships between heat transfer coefficient, temperature, solid fraction of droplets and the flight distance for each droplet of 10, 20, 40, 60, 80, 120 μm in diameter are shown in Fig. 3. Droplet heat transfer coefficient decreases with increasing droplet velocity to the minimum value $2k_g/d$, then rises with decreasing droplet velocity as shown in Fig. 3a. The change of droplet temperature can be divided into five stages as shown in Fig. 3b. The temperature to start with segregation is 907-995K. The solid fraction of droplet due to recalescence is nearly 1.2% which is determined by the degree of undercooling. During eutectic solidification, solid fraction is about 8.8% for all the droplets as shown in Fig. 3c.

The heat transfer coefficient for a droplet of 10 μm increased to 9017 $Wm^{-2}K^{-1}$ compared with 1588.1 $Wm^{-2}K^{-1}$ for a droplet of 120 μm in diameter. Thus the total solidification time for a droplet of 10 mm is decreased by 0.1913 s compared with 0.6581 s for a droplet of 120 μm in diameter. This behavior indicates that a smaller droplet can obtain a higher heat transfer coefficient and a lower temperature, solidify completely at a much shorter flight time from the nozzle and experience a higher cooling rate, which is attributable to the fact that the droplet has a smaller surface area for heat transfer.

3.2. Effects of initial gas velocity

The relationships between gas/droplet slip velocity, droplet velocity, heat transfer coefficient, temperature, solid fraction, and spray distance for

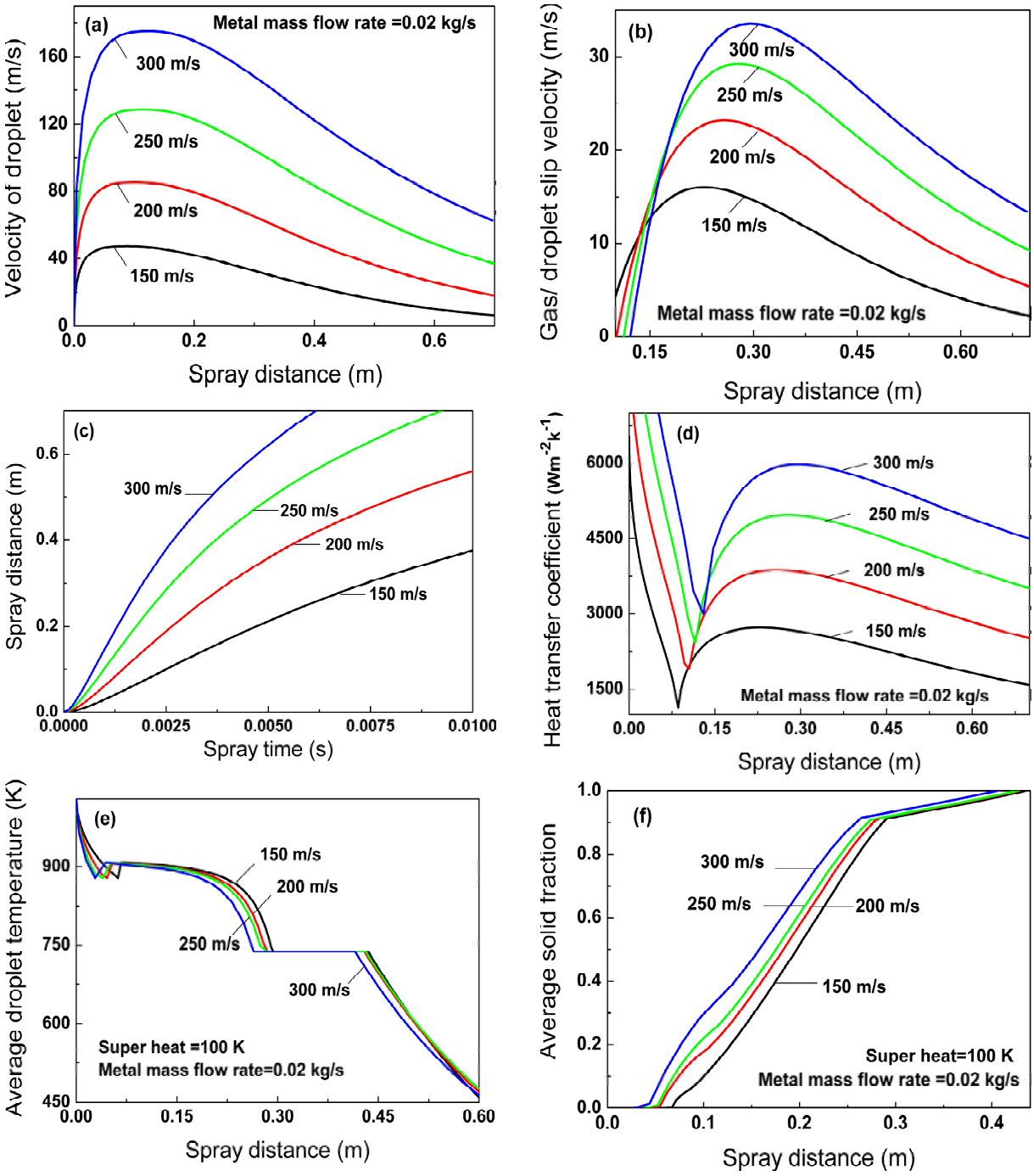

Fig. 4. Variations of droplet velocity (a), slip velocity (b), flight distance (c), heat transfer coefficient (d), droplet temperature (e), and solid fraction (f) for different initial gas velocities.

each initial gas velocity of 150 m/s, 200 m/s, 250 m/s, and 300 m/s are shown in Fig. 4.

Droplet velocity and gas/droplet slip velocity increase with increasing initial gas velocity and spray distance and reach higher maximum values in shorter spray distances as shown in Figs. 4a and 4b. For example, with initial metal mass flow rate of 0.02 kg/s, the maximum velocity of droplet for an initial velocity 300 m/s increases by 175.225 m/s compared with that of an initial gas velocity of 150 m/s. In addition, the droplet spray distance at the maximum velocity for an initial gas velocity 300 m/s increases by 0.1297 m compared with 0.0858 m for an initial gas velocity of 150 m/s. Fig 4c illustrates the relationship between spray time and spray distance.

The temperature variation of the droplets is shown in Fig. 4e, which manifests obvious effect of initial

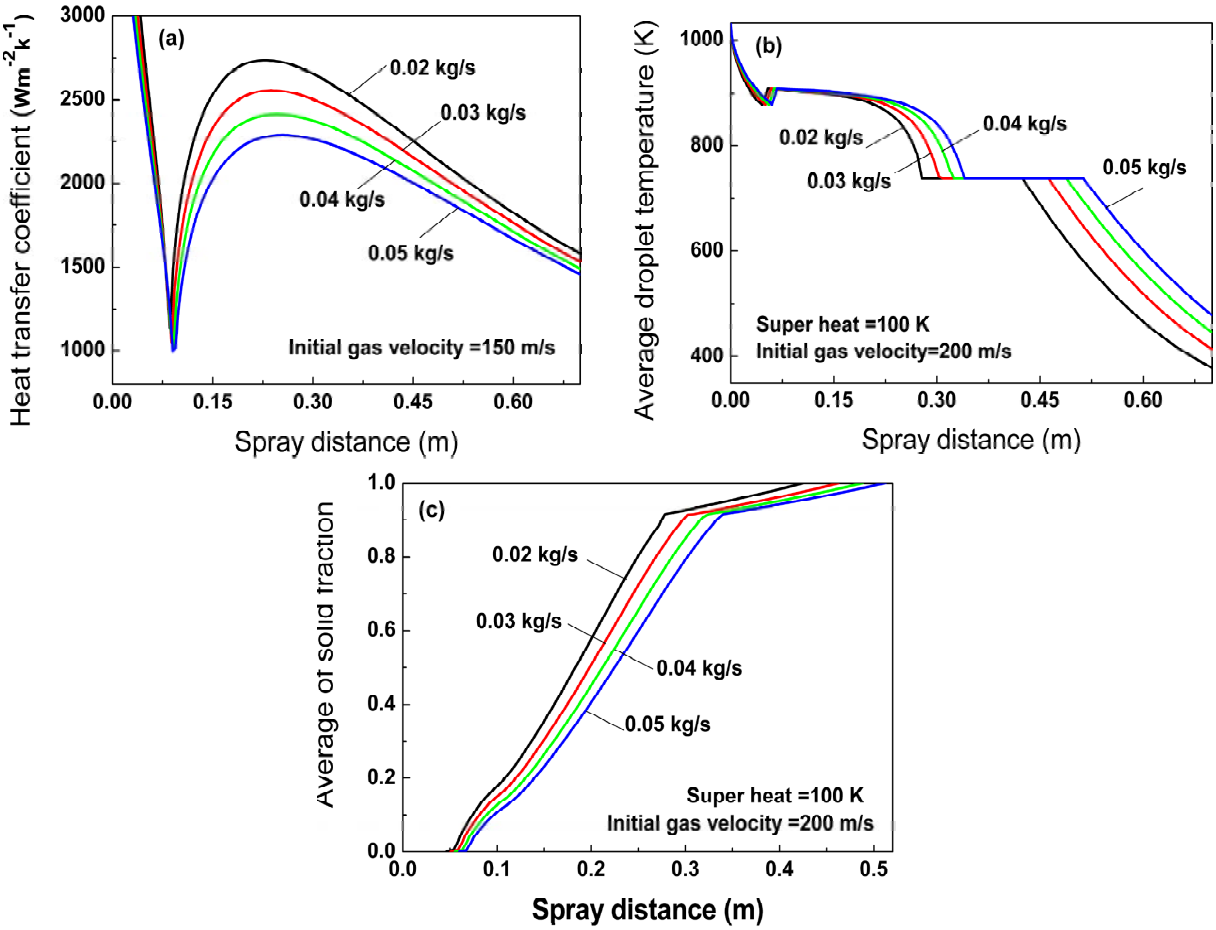

Fig. 5. Variations of droplet heat transfer coefficient (a), temperature (b), and average solid fraction (c) for different metal mass flow rates.

gas velocity. From the trajectory, it seems that the temperature decreases with increasing initial gas velocity. The change of temperature is directly related to the heat transfer coefficient. The heat transfer coefficient at the spray distance of 0.3 m for an initial gas velocity 300 m/s increases by about 50% compared with that for an initial gas velocity of 150 m/s as shown in Fig. 4d. But the temperature changes little because there is not enough time for heat transfer. The droplet with a higher velocity can finish solidification earlier as shown in Fig. 4f.

3.3. Effects of metal mass flow rate

Fig. 5 shows droplet heat transfer coefficient, droplet temperature, solid fraction as functions of spray distance from the atomizer with different metal mass flow rates of 0.02 kg/s,0.03 kg/s, 0.04 kg/s, 0.05 kg/s, respectively. As shown in Fig. 5, the heat transfer coefficient at the spray distance of 0.3 m for a metal mass flow rate for 0.05 kg/s decreases by 2262 $Wm^{-2}K^{-1}$ compared with 2653 $Wm^{-2}K^{-1}$ for a metal mass flow rate of 0.02 kg/s. Solid fraction decreases with increasing metal mass flow rate. This is attributed to decreasing heat transfer coefficient between droplet and gas around the droplet.

4. CONCLUSIONS

In the spray rolling process of 7050 aluminum alloy, in order to predict the effects of droplet diameter, initial gas velocity, metal mass flow rate and flight distance on gas/droplet slip velocity, droplet velocity ,the heat transfer coefficient, solid fraction and droplet temperature, the Newtonian heat transfer formulation has been coupled with the special solidification process. The droplet cooling rate during spray can be controlled effectively by adjusting the initial gas velocity, metal mass flow rate and droplet flight time by changing the enthalpy of the spray to reduce the porosity of deposits and the risk of hot cracking. A small droplet can have a higher heat transfer coefficient than a larger droplet, solidify completely in a shorter time and experiences a higher cooling rate. Droplet velocity, heat transfer coefficient

and solid fraction increase and droplet temperature decreases when the initial gas velocity increases. When metal mass flow rate increases, droplet heat transfer coefficient, droplet velocity, heat transfer coefficient and average solid fraction decrease, but droplet temperature increases.

ACKNOWLEDGEMENTS

The authors gratefully acknowledge the financial support of National Natural Science Foundation of China (Project No. 50774035) and the Fundamental Research Funds for the Central Universities (Grant No. 2011ZZ0010).

REFERENCES

[1] K.M. McHugh, E.J. Lavernia, Y. Zhou, Y. Lin, J.-P. Delplanque and S.B. Johnson, In: *SDMA 2003 and ICSF V*, ed. by K.Bauckhage, U. Fritsching, V.Uhlenwinkel, J.Ziesenis and A. Leatham (Bremen, Germany, 2003), p. 22.

[2] K.M. McHugh, Y. Lin, Y. Zhou, S.B. Johnson, J.-P. Delplanque and E.J. Lavernia // *Mater. Sci. Eng. A* **477** (2008) 26.

[3] K.M. McHugh, J.-P. Delplanque, S.B. Johnson,E.J. Lavernia, Y. Zhou and Y. Lin // *Mater. Sci. Eng.* **383** (2004) 96.

[4] J.W. Rogers // *Sci. Tec. Pro.* **1** (2005) Number 1.

[5] J.-P. Delplanque, E.J. Lavernia and R.H. Rangel // *Numerical Heat Transfer* **30A** (1996) 1.

[6] J.-P. Delplanque, E.J. Lavernia and R.H. Rangel // *J. Heat Transfer* **122** (2000) 126.

[7] S.B. Johnson, J.P. Delplnque, E.J. Lavernia, Y. Zhou,Y. Lin and K.M. McHugh, In: *Symposium on Hot Deformation of Aluminum Alloys, 132nd TMS Annual Meeting & Exhibition* (San Diego, March 2003), p. 2.

[8] N. Zeoli and S. Gu // *Comput. Mater. Sci.* **43** (2008) 268.

[9] M. Garbero, M. Vanni and U. Fritsching // *Int. J. Heat and Fluid Flow* **27** (2006) 105.

[10] S.B. Johnson, J.P. Delplanque, Y.J. Lin, Y. Zhou, E.J. Lavernia and K.M. McHugh, In: *SDMA 2003 and ICSF V*, ed. by K. Bauckhage, U. Fritsching, V. Uhlenwinkel, J. Ziesenis and A. Leatham (Bremen, Germany, 2003), p. 6-3.

[11] Y. Lin, Y. Zhou, S.B. Johnson, J.-P. Delplanque , K.M. McHugh and E.J. Lavernia, In: *SDMA 2003 and ICSF V*, ed. by K.Bauckhage,U. Fritsching, V.Uhlenwinkel, J.Ziesenis and A. Leatham (Bremen, Germany, 2003), p. 7-17.

[12] K.M. McHugh, J.E. Folkestad, In: *SDMA 2003 and ICSF V*, ed. by K.Bauckhage, U. Fritsching, V. Uhlenwinkel, J. Ziesenis and A. Leatham (Bremen, Germany, 2003), p. 5-123.

[13] Y.J. Lin, K.M. McHugh, Y. Zhou and E.J. Lavernia // *Metall. Mater. Trans. A* **35** (2004) 3595.

[14] Y. Lin, K. M. McHugh Y. Zhou and E.J. Lavernia // *Metall. Mater. Trans. A* **35** (2004) 3633.

[15] K.M. McHugh, E.J. Lavernia , Y. Zhou, Y. Lin, J.-P. Delplanque and S.B. Johnson, In: *SDMA 2003 and ICSF V*, ed. by K.Bauckhage,U. Fritsching, V.Uhlenwinkel, J.Ziesenis and A. Leatham, (Bremen, Germany, 2003), p. 6-27.

[16] P. Mathur, D. Apelian and Lawley // *Acta Metall. Mater.* **37** (1989) 429.

[17] P.S. Grant, B. Cantor and Katgerman // *Acta Metall. Mater.* **41** (1993) 3097.

[18] B.P. Bewlay and B. Cantor // *Metall. Mater. Trans. B* **21** (1990) 899.

[19] E. Lee, K.H. Kim and S. Ahn // *Proc. Powder Metal.* (1993) 35.

[20] E. Lee and S. Ahn // *Acta Metal. Mater.* **42** (1994) 3231.

[21] J.-P. Delplanque, S.B. Johnson, Y. Lin, Y. Zhou, N. Yang, K.M. McHugh and E.J. Lavernia, In: *Proc. Int. Conf. Process Modeling in Powder Metallurgy & Particulate Materials* (Newport Beach, CA 2002), p.28.

[22] D.E. Lawrynowicz, B. Li. and E.J. Lavernia // *Metall. Mater. Trans. B* **28** (1997) 877.

[23] U. Fritsching, D. Bergmann and K. Bauckhage, In: *Proc. Int. Conf. Liquid Atomization and Spray Systems* (ICLASS 1997), p.18

[24] C.G. Levi and R. Mehrabian // *Metall. Trans. A* **13** (1982) 221.

[25] E.J. Lavernia, G.M. Gutierrez, J. Szekely and N.J. Grant // *Int. J. Rapid Solid.* **4** (1988) 89.

[26] W.E. Ranz and W.R. Marshall // *Chem. Eng. Prog.* **48** (1952) 141.

[27] M.C. Flemings, *Solidification Processing* (McGraw-Hill, New York, 1974).

[28] T.P. Battle // *Int. Mater. Rev.* **37** (1992) 249.